Review

Catalytic prenylation and reverse prenylation of aromatics

Yan-Cheng Hu, [1,2] Xiang-Ting Min, [1] Ding-Wei Ji, [1] and Qing-An Chen ![ORCID] [1,2,*]

Prenylated and reverse-prenylated aromatics are present in numerous natural terpenoids with a broad spectrum of pharmaceutical activity. In their biosynthesis, prenyl and reverse-prenyl motifs are selectively introduced via enzyme catalysis with dimethylallyl pyrophosphate (DMAPP) and isopentenyl pyrophosphate (IPP) as the precursors. In recent years, considerable efforts have been devoted to emulating the biological process with chemical catalysis via the intermediacy of π-prenyl species. A set of elegant strategies including the Friedel–Crafts reaction, cross-coupling, C–H activation, Tsuji–Trost-like reactions, addition reactions, and radical coupling have been demonstrated. This review aims to highlight these advances and discuss the regioselectivity issues, which will definitely further expand their applications and promote the development of this field.

Introduction to prenylation and reverse prenylation of aromatics

Prenylation and reverse prenylation are essential steps for the synthesis of terpenoids that are omnipresent in nearly all living organisms [1,2]. The prenyl and reverse-prenyl units can increase the lipophilicity and binding affinity with target proteins. Prenylated and reverse-prenylated aromatics represent one of the most important class of terpenoids that usually display a broad range of medicinal properties including antibiotic [3], antibacterial [4], antioxidant [5], antimalarial [6], and anticancer [7] activities (Figure 1A). In nature, DMAPP and IPP, obtained via the mevalonate (MVA) and methylerythritol 4-phosphate (MEP) pathways, are used as the donors for the incorporation of prenyl and reverse-prenyl motifs on aromatics (Figure 1B). The site selectivity and regioselectivity are manipulated by the choice of prenyltranferases (PTs), which generally chelate with divalent cations (e.g., Mg^{2+}) [8]. Mg^{2+} can further coordinate with pyrophosphate groups to promote the formation of π-prenyl carbocation and subsequent attack of the aromatics leads to prenylation or reverse prenylation.

Owing to the fundamental importance of prenylation and reverse prenylation, the emulation of biological processes with chemical catalysis involving the intermediacy of π-prenyl species has gained much attention. According to the mechanisms, strategies include the Friedel–Crafts reaction, cross-coupling, C–H bond activation, Tsuji–Trost-like reactions, addition reactions, and radical coupling (Figure 1C). Nevertheless, most have been studied randomly in the development of allylations. Therefore, there is an urgent need to give a specific summary on this state-of-the-art topic. This review primarily focuses on the direct prenylation and reverse prenylation of aromatics enabled by chemical catalysis and is organized by catalytic strategy.

Catalytic prenylation of aromatics via Friedel–Crafts reaction

In biosynthesis, enzymatic prenylation and reverse prenylation include two steps: Mg^{2+}-assisted formation of a π-prenyl cation-pyrophosphate ion pair and subsequent nucleophilic attack of aromatics [9]. Emulating this Friedel–Crafts-type mechanism, Menéndez and colleagues attempted biomimetic synthesis of indole alkaloid tryprostatin B (Figure 2A) [10]. When using magnesium

Highlights

Prenylation and reverse prenylation are omnipresent in nearly all living organisms. In nature, these fundamental reactions rely on enzyme catalysis with dimethylallyl pyrophosphate (DMAPP) as the donor.

Emulating biological process with chemical catalysis provides new opportunities to achieve prenylation and reverse prenylation of aromatics. The strategies include the Friedel–Crafts reaction, cross-coupling, C–H activation, the Tsuji–Trost reaction, addition reactions, and radical coupling.

Because of the steric hindrance, prenylation is achieved in most cases, whereas reverse prenylation can be attained via Suzuki cross-coupling and the Tsuji–Trost reaction.

From the viewpoint of step and atom economy, basic feedstock isoprene is an ideal donor for the incorporation of prenyl and reverse-prenyl groups. The regioselectivity can be diverted through modulation of the transition metals and ligands.

[1]Dalian Institute of Chemical Physics, Chinese Academy of Sciences, 457 Zhongshan Road, Dalian 116023, China
[2]University of Chinese Academy of Sciences, 19 A Yuquan Road, Shijingshan District, Beijing 100049, China

*Correspondence:
qachen@dicp.ac.cn (Q.-A. Chen).

nitrate as additive, a tryptophan-based dipeptide (cyclo-L-Trp-L-Pro) could react with prenyl bromide in acetic acid buffer, giving rise to a mixture of C3 prenylated diastereomers (**7a** and N-prenylated **9a**) and the C2 prenylated product tryprostatin B (**8a**). With the aid of NaOAc, this reaction also proceeded smoothly in acetic acid (Figure 2A) [11]. However, it should be noted that, in this case, tryprostatin B **8a** cannot be separated from the C3 prenylated product **7a** because of their similar polarities. Thus, the selective incorporation of a prenyl group at the C2 position of indoles often relies on the use of stoichiometric promoters [12–14]. For example, Danishefsky and colleagues demonstrated that tryptophanate easily reacted with tert-butyl hypochlorite to afford reactive intermediate 3-chloroindolenine, which could further undergo C2 prenylation with prenylstannane in the presence of BCl_3 (Figure 2B) [12].

In comparison, Chen's group recently achieved C2 prenylation of 3-substituted indoles via the Friedel–Crafts reaction (Figure 2C) [15]. With tert-prenol **2b** as a partner and $AlCl_3$ as a catalyst, tryptophol was converted to its C2-prenylated product **10a** in a reasonable yield, while solid acid Nafion resin was an optimal catalyst for prenylation of bioactive melatonin (**10b**). Notably, the dipeptide Fmoc-L-Pro-L-Trp-OMe participated in this prenylation as well, resulting in the formation of product **10c** at 40% yield. Furthermore, the coupling of 3-prenylindole and deuterated tert-prenol (**2b–d**) gave rise to a mixture of **10d** and **10d'**. This result suggests that both direct C2 prenylation and tandem C3 prenylation/migration pathways may be involved in this Friedel–Crafts reaction.

The Friedel–Crafts reaction of anisole with prenyl acetate was executed by a molybdenum(II) complex $[Mo(CO)_4Br_2]_2$, providing a mixture of para and ortho isomers (**12a**) (Figure 2D) [16]. With Lewis acid $Bi(OTf)_3$ as a catalyst, isoprene was also a good prenyl donor for electron-rich 1,2,3-trimethoxybenzene (**12b**) [17]. Interestingly, $Bi(OTf)_3$-catalyzed coupling between 1,2-dimethoxybenzene and isoprene in $MeNO_2$ afforded an annulative product (**12c**) [18]. The transformation proceeds through a domino prenylation and intramolecular cyclization process. A combination of $FeCl_3$ and $AgBF_4$ also exhibited good catalytic performance towards the prenylation of electron-rich arenes with isoprene (**12d–f**) [19].

In 2010, Niggemann and colleagues disclosed that 1,3-dimethoxybenzene underwent Friedel–Crafts prenylation readily with tert-prenol (**12g**) when assisted by $Ca(NTf_2)_2$ and nBu_4NPF_6 catalysts (Figure 2D) [20]. Later, a metal-free alternative was developed by Hall and coworkers in which bench-stable boronic acid served as the catalyst [21]. For example, in the presence of tetrafluorophenylboronic acid (**A1**), 4-methylphenol was a viable substrate (**12h**) and no further O-cyclized product was obtained. Moreover, dimethylallene proved to be an effective donor for prenylation of 1,3,5-trimethoxybenzene under gold catalysis (**12i**) [22].

While some progress has been achieved, only electron-rich aromatics were suitable substrates and sometimes it is difficult to control the site selectivity. Besides, as nucleophiles favorably attack at the less-hindered terminal position, prenylated products are generally obtained. This area can be directed further towards the development of enantioselective prenylation of 3-substituted indoles with chiral phosphoric acids.

Catalytic prenylation and reverse prenylation of aromatics via cross-coupling

Transition-metal-catalyzed cross-couplings of aryl organometals with unsubstituted or aryl-substituted allylic electrophiles have been well investigated [23–27]. However, this strategy cannot be simply extended to prenylation reactions. Linear/branched selectivity is often encountered and is more difficult to tackle than with common allylations. For instance, the use of prenyl electrophiles often leads to a mixture of linear (prenyl) and branched (reverse prenyl) regioisomers
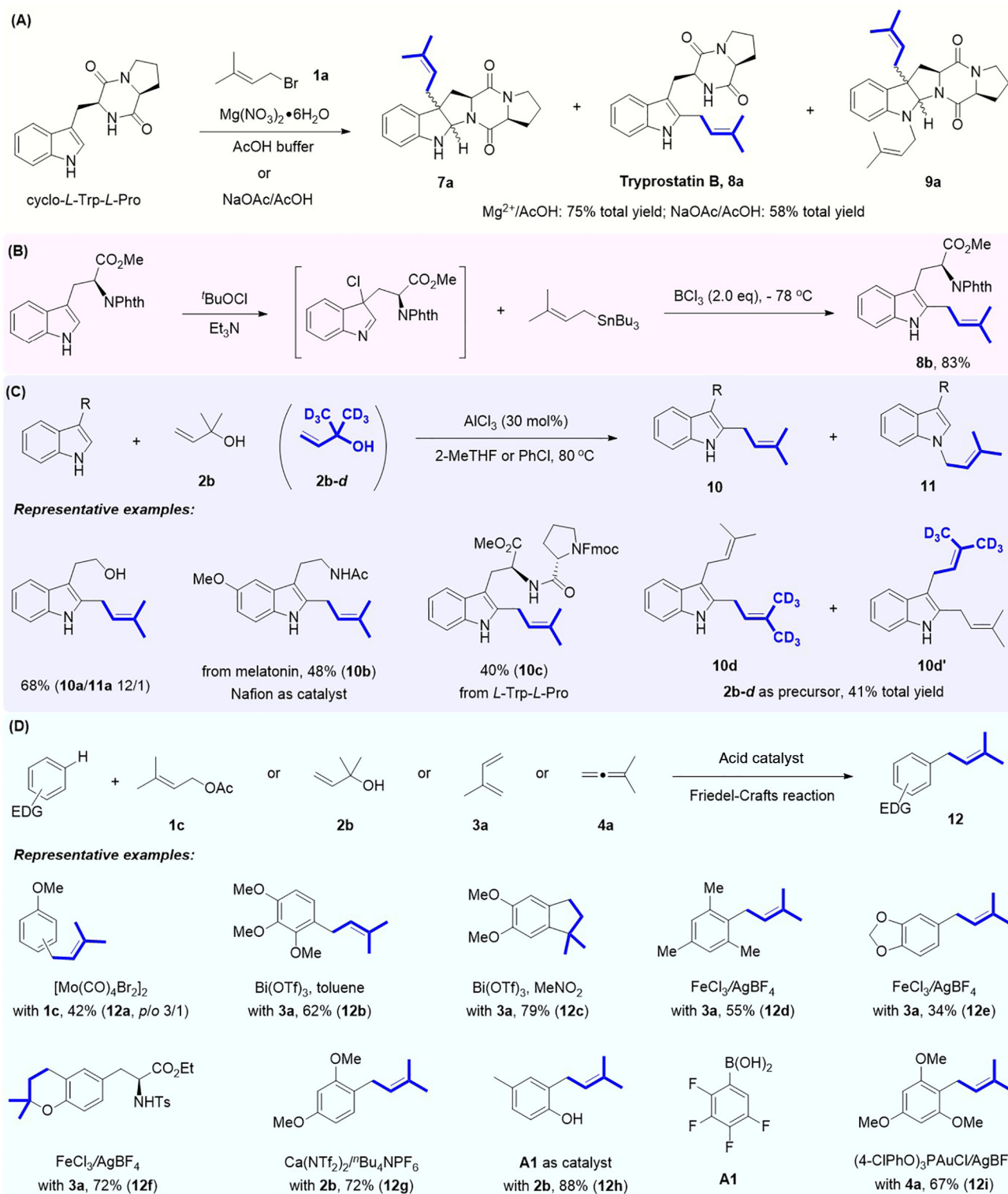
Figure 1. Catalytic prenylation and reverse prenylation of aromatics. (A) Representative bioactive natural (reverse-)prenylated aromatics. (B) Prenylation and reverse prenylation of aromatics via enzyme catalysis. (C) Prenylation and reverse prenylation of aromatics via chemical catalysis. Abbreviations: CoA, coenzyme A; DG, directing group; DMAPP, dimethylallyl pyrophosphate; IPP, isopentenyl pyrophosphate; LG, leaving group; MEP, methylerythritol 4-phosphate; MVA, mevalonate.

[28–31]. This is likely to be because there exists an equilibrium between linear and branched σ-prenyl-metal intermediates and the subsequent steps (transmetalation/reductive elimination) of the two isomers might have similar rates. Currently, the prenylation of arenes is often achieved by Pd-catalyzed coupling of arylhalides and prenyl organometals.

A variety of prenyl reagents including prenyl stannane [32,33], trifluorosilane [34,35], boronate [36], indium [37,38], and zinc [39–41] are suitable donors (Figure 3A). The commonly used palladium catalysts such as $Pd(PPh_3)_4$, $PdCl_2(dppf)$, and $PdCl_2(PPh_3)_2$ can promote these couplings. In these protocols, the linear-type σ-prenyl-Pd-Ar intermediate, generated by transmetalation between Ar-Pd-X and prenyl organometals, is likely to undergo a rapid reductive elimination to yield the prenylated products. Pd-prenyl is sensitive to base-induced elimination, and as a result weakly or non-basic reagents are generally used. Some well-defined palladium complexes also showed excellent catalytic performance towards prenylation. For instance, the N-heterocyclic carbene (NHC)-based palladium complex Pd-PEPPSI-IPent, developed by Organ's group, could catalyze cross-coupling between aryl halides and prenyl boronate/zinc pivalate [39,40]. The bulky nature of the catalyst can accelerate the reductive elimination step to enhance the efficiency. With complex CPhos-Pd-G3, prenylzinc bromide was effectively coupled with aryl bromide at room temperature, furnishing the prenylarenes in good yields [41].

(A)

cyclo-*L*-Trp-*L*-Pro

1a

Mg(NO₃)₂·6H₂O
AcOH buffer
or
NaOAc/AcOH

7a + Tryprostatin B, **8a** + **9a**

Mg²⁺/AcOH: 75% total yield; NaOAc/AcOH: 58% total yield

(B)

^{t}BuOCl
Et₃N

BCl₃ (2.0 eq), − 78 °C

8b, 83%

(C)

2b **2b-*d***

AlCl₃ (30 mol%)
2-MeTHF or PhCl, 80 °C

10 + **11**

Representative examples:

68% (**10a/11a** 12/1)

from melatonin, 48% (**10b**)
Nafion as catalyst

40% (**10c**)
from *L*-Trp-*L*-Pro

10d + **10d'**

2b-*d* as precursor, 41% total yield

(D)

EDG +
1c or **2b** or **3a** or **4a**

Acid catalyst
Friedel-Crafts reaction

12

Representative examples:

[Mo(CO)₄Br₂]₂
with **1c**, 42% (**12a**, *p/o* 3/1)

Bi(OTf)₃, toluene
with **3a**, 62% (**12b**)

Bi(OTf)₃, MeNO₂
with **3a**, 79% (**12c**)

FeCl₃/AgBF₄
with **3a**, 55% (**12d**)

FeCl₃/AgBF₄
with **3a**, 34% (**12e**)

FeCl₃/AgBF₄
with **3a**, 72% (**12f**)

Ca(NTf₂)₂/^{n}Bu₄NPF₆
with **2b**, 72% (**12g**)

A1 as catalyst
with **2b**, 88% (**12h**)

A1

(4-ClPhO)₃PAuCl/AgBF₄
with **4a**, 67% (**12i**)

Trends in Chemistry

(See figure legend at the bottom of the next page.)

In 2013, Buchwald and colleagues demonstrated that, for [(allyl)PdCl]$_2$-catalyzed Suzuki coupling, divergent regioselectivity could be attained through the choice of ligand (Figure 3B) [42]. Prenylarenes were produced with sterically demanding ^{t}BuXPhos, whereas the pathway was altered to reverse prenylation on varying of the ligand to **L1**. It should be mentioned that when *tert*-prenyl boronate was used as a donor, the prenylation also occurred with excellent selectivity, illustrating that the interconversion of two σ-prenyl-Pd-Ar isomers via π-prenyl-Pd-Ar (**INT-1**) is a fast step. With bulky ligand ^{t}BuXPhos, less-hindered linear σ-prenyl-Pd-Ar is favored. This bulky ligand can also facilitate the following reductive elimination step. By contrast, a low selectivity was obtained for reverse prenylation with *tert*-prenyl boronate, which is likely to be because two σ-prenyl-Pd isomers do not reach equilibrium before reductive elimination occurs.

Later, Knölker and coworkers accomplished an interesting Pd-catalyzed prenylation and reverse prenylation of bromocarbazole through tuning of the (*tert*-)prenyl precursors (Figure 3C) [43]. With prenyl stannane or boronate as a partner, the coupling furnished a reverse-prenylated product in the presence of Pd(dba)$_2$ and ^{t}Bu$_3$P. However, varying the donor to *tert*-prenyl stannane or boronate enabled a selective introduction of a prenyl group onto bromocarbazole.

These efficient cross-couplings have found wide applications in the synthesis of natural products (Figure 3D). For example, the prenyl group in the bioactive molecules V-ATPase inhibitor [44], demethylasterriquinone B1 [45], and nodulisporic acid C [46] was installed via Stille cross-coupling. The broad applicability of Suzuki prenylation was highlighted in the preparation of glycybenzofuran [47], myrsinoic acid F [48], clavicipitic acid [49], cyclopiazonic acid [50], and griseofamine A [51]. By using Buchwald's reverse-prenylation protocol, Reisman and colleagues established the enantioselective synthesis of the alkaloid lansai B [52].

In 2006, Yorimitsu and Oshima and colleagues unveiled an interesting Pd(OAc)$_2$/PCy$_3$-catalyzed prenyl transfer from homoallyl alcohol **6a** to aryl halides (Figure 4A) [53,54]. An initial oxidative addition and ligand exchange with homoallyl alcohol produce intermediate **INT-2**. A further retro-prenylation via a six-membered transition state yields the σ-prenyl-Pd-Ar species **INT-3**, followed by reductive elimination to obtain prenylarenes. Remarkably, congested 2-bromo-1,3-dimethylbenzene participated in the prenylation well (**13b**), which is likely to be because the steric repulsion around the palladium center can accelerate the rate-determining retro-prenylation step.

Besides traditional Pd(0) catalysis, Sawamura and coworkers accomplished the first Pd(II)-catalyzed coupling of phenylboronic acid and *tert*-prenyl acetate with the help of a 1,10-phenanthroline (phen) ligand and AgSbF$_6$ (Figure 4B) [55,56]. Alternatively, a neutral Pd(II)-dimer complex, prepared from Pd(OAc)$_2$ and sulfonamidoquinoline ligand, was an effective catalyst as well [57]. The process starts with the transmetalation between cationic Pd(II) species and phenylboronic acid. Subsequent acetate-directed alkene insertion into Pd-phenyl (**INT-6**) and **β-oxygen elimination** (see Glossary) produce prenylbenzene **13d**.

In 2013, Gong and his colleagues disclosed an Ni-catalyzed reductive coupling of 5-bromo-1,2,3-trimethoxybenzene with prenyl acetate (Figure 4C) [58]. A combination of pyridinylimidazole ligand **L2** and pyridine was critical for the transformation. Later, Shu and colleagues reported a reductive prenylation using *tert*-prenol with Ni(dppf)Cl$_2$/AlCl$_3$ as catalysts and manganese as reductant [59]. In this case, Me$_4$-phen **L3** was the optimal ligand. In Gong's work, the reaction

Figure 2. Catalytic Friedel–Crafts prenylation of aromatics. (A) Biomimetic synthesis of natural indole alkaloid tryprostatin B. (B) C2 prenylation of tryptophanate promoted by ^{t}BuOCl and BCl$_3$. (C) AlCl$_3$-catalyzed C2 prenylation of 3-substituted indoles. (D) Lewis-acid-catalyzed prenylation of electron-rich aromatics. Abbreviations: 2-MeTHF, 2-methyl tetrahydrofuran; EDG, electron-donating group; Phth, phthaloyl.
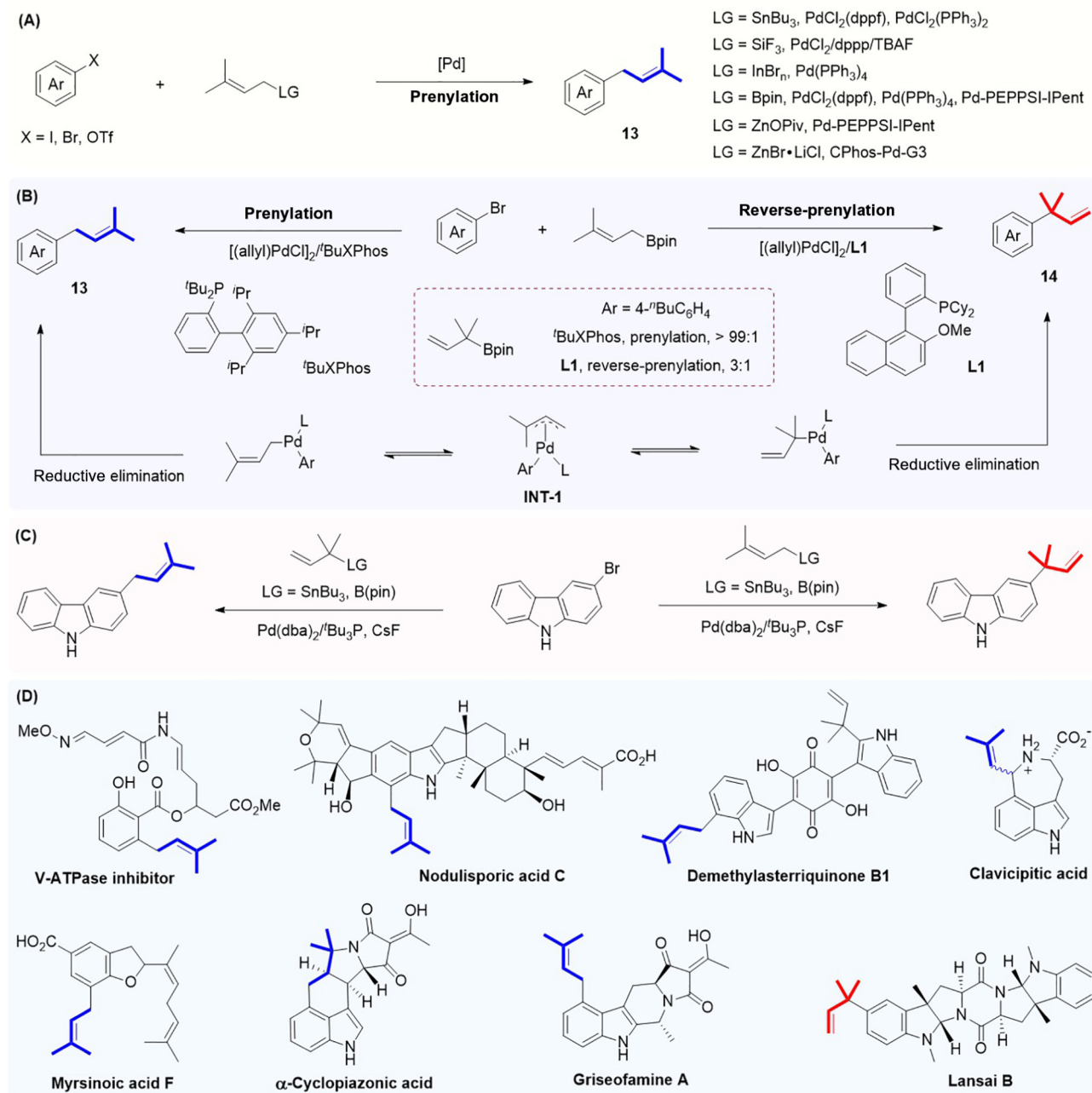
Figure 3. Catalytic prenylation and reverse prenylation of aromatics via cross-coupling. (A) Pd-catalyzed prenylation of aryl halides with various prenylmetal reagents. (B) Switchable regioselectivity controlled by catalysts. (C) Switchable regioselectivity controlled by (*tert*-)prenyl precursors. (D) Representative natural products whose synthesis relies on prenylation and reverse prenylation of aromatics via cross-coupling. Abbreviations: Bpin, pinacolateboryl; CPhos-Pd-G3, {[2-dicyclohexylphosphino-2',6'-bis(*N*,*N*-dimethylamino)-1,1'-biphenyl]-2-[2'-amino-1,1'-biphenyl]} palladium(II) methanesulfonate (CAS: 1447963-73-6); dba, dibenzylideneacetone; dppf, 1,1'-ferrocenediyl-bis(diphenylphosphine); dppp, 1,3-bis(diphenylphosphino)propane; Pd-PEPPS-IPent, [1,3-bis(2,6-di-3-pentylphenyl)imidazol-2-ylidene](3-chloropyridyl)palladium(II) dichloride (CAS: 1158652-41-5); TBAF, tetrabutylammonium fluoride.
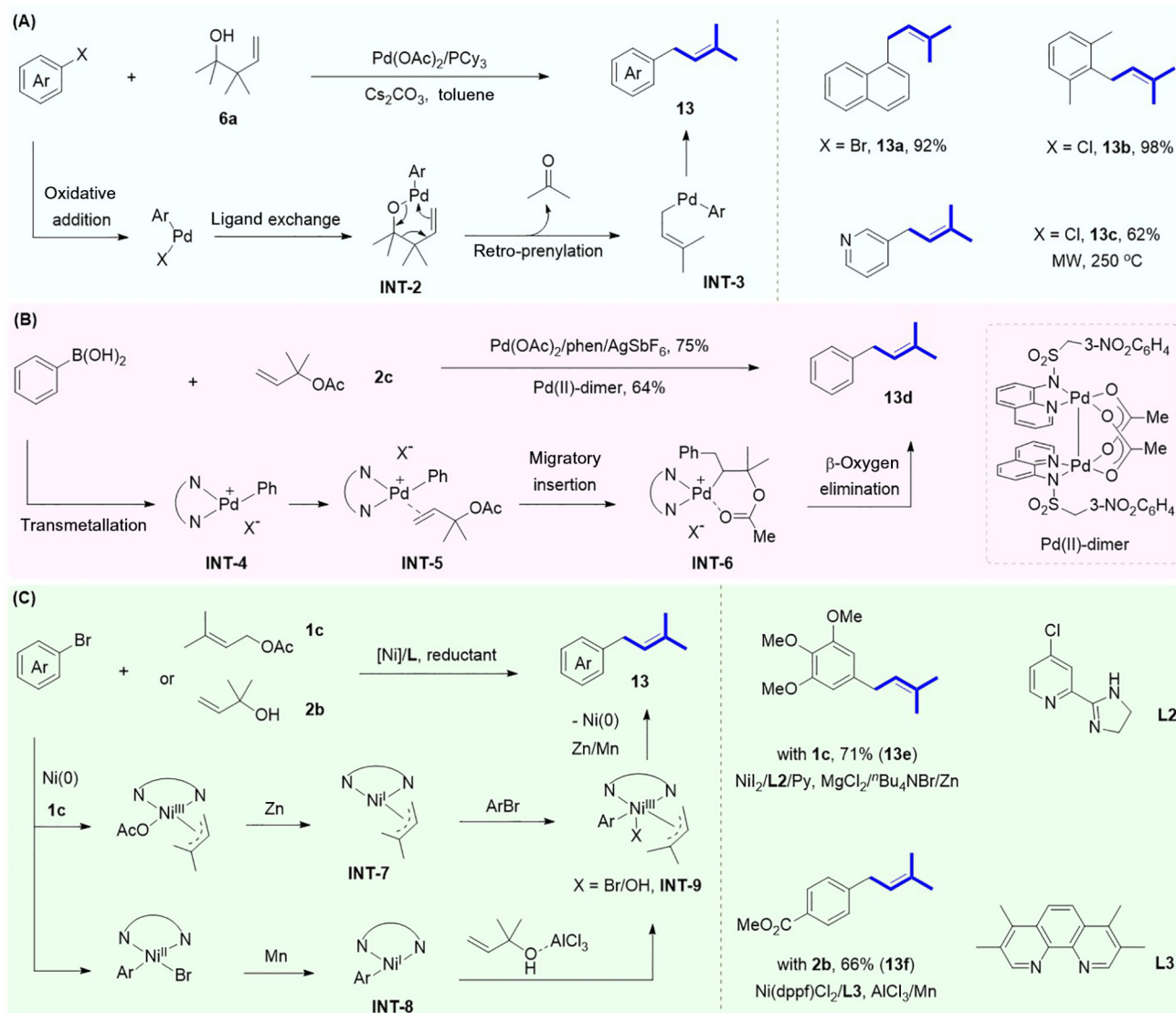
Figure 4. Catalytic prenylation and reverse prenylation of aromatics via cross-coupling. (A) Pd-catalyzed prenylation of aromatics using homoallyl alcohol. (B) Pd(II)-catalyzed coupling of phenylboronic acid and *tert*-prenylacetate. (C) Ni-catalyzed reductive phenyl–prenyl cross-coupling. Abbreviation: phen, 1,10-phenanthroline.

starts with oxidative addition between Ni(0) and prenyl acetate, followed by reduction with Zn to generate the prenyl-Ni(I) complex **INT-7**. By comparison, Shu and colleagues proposed that the process is initiated by oxidative addition of Ni(0) with aryl bromide and subsequent reduction with Mn. The formed Ar-Ni(I) intermediate **INT-8** further undergoes oxidative addition with activated (*tert*-)prenol to deliver Ar-Ni(III)-prenyl (**INT-9**). This species can also be produced via oxidative addition of **INT-7** with aryl bromide. Then, reductive elimination of **INT-9** affords the expected product and the eventual reduction of Ni(I) species with Zn/Mn regenerates the Ni(0) catalyst.

Catalytic prenylation and reverse prenylation of aromatics via C–H activation

In 2009, Baran and coworkers described a Pd(OAc)$_2$-mediated oxidative coupling between 3-substituted NH indoles and 2-methyl-2-butene for the facile synthesis of *N*-reverse-

prenylated indoles (Figure 5A) [60]. Besides AgTFA and Cu(OAc)$_2$ as oxidants, additional stabilizing ligands 3-NO$_2$-pyridine and methyl acrylate were required for the reaction of electron-deficient indoles (**15a,b**). The amine protecting groups, including Fmoc, Boc, and Phth on *L*-tryptophanate, were all tolerated (**15c–e**). Notably, *L*-tryptophan-derived dipeptide and tripeptide were accommodated to this transformation as well (**15f,g**). Mechanistically, Pd(OAc)$_2$-assisted allylic C–H activation of 2-methyl-2-butene first occurs, resulting in the formation of the π-prenyl-Pd complex **INT-10**. Subsequent ligand exchange with NH indole (**INT-11**) and reductive elimination yield the final product. Another possibility includes palladation at the C3 position of indole and following metallo-Claisen rearrangement (**INT-12**). The resulting Pd(0) species is finally oxidized by Ag(I) and Cu(II) to complete the cycle. More importantly, the utility of this strategy has been highlighted by its implementation in the total synthesis of various alkaloids, such as emindole PB [61], rufomyazine [62], ilamycin E$_1$ [63], and desoxycyclomarin C [64] (Figure 5B).
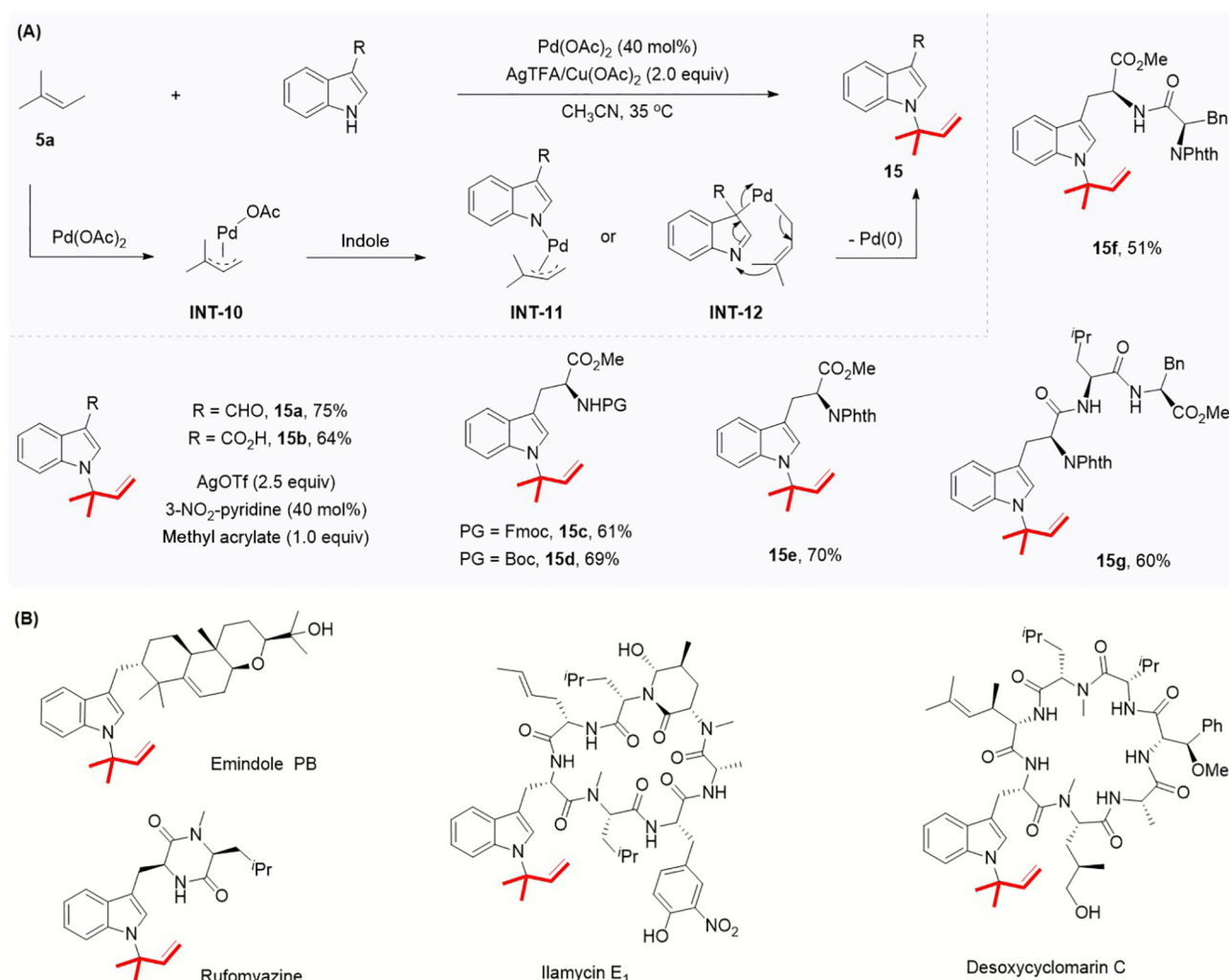

Figure 5. Catalytic prenylation and reverse prenylation of aromatics via C–H activation. (A) Pd(OAc)$_2$-catalyzed *N*-reverse prenylation of indoles with 2-methyl-2-butene. (B) Representative alkaloids whose synthesis relies on *N*-reverse prenylation of indoles. Abbreviations: Boc, *tert*-butoxycarbonyl; Fmoc, 9-fluorenylmethoxycarbonyl; Phth, phthaloyl.

Directed C–H bond activation is another feasible strategy to incorporate a prenyl group on the aromatics (Figure 6A). Under cationic Rh(III) catalysis, pyridine [65], trichloroacetimidamide [66], amide [67], and thiazole [68] were effective directing groups to facilitate C–H prenylation of aromatics. The cationic Ru(II) [69,70] and Co(III) [71–73] systems were able to execute C2 prenylation of indoles (**16b,c**) and pyrrole (**16d**) using *tert*-prenol **2b** as the donor. Ackermann and coworkers disclosed that with a Mn$_2$(CO)$_{10}$ catalyst, phenyl ketimine could be coupled with *tert*-prenyl carbonate **2d**, and subsequent *in situ* hydrolysis produced prenylated acetophenone (**16e**) [74]. In general, the mechanism for directed C–H prenylation includes five-membered metallacycle formation via a **concerted metalation-deprotonation (CMD)**-type C–H activation pathway, migratory insertion of olefin into a metal-carbon bond (**INT-13**) and β-oxygen elimination.

In 2015, Chen and colleagues developed a Pd(OAc)$_2$-catalyzed, aminoquinoline (AQ)-directed C–H prenylation of aromatic (**16f**) with prenyl bromide in the presence of (BnO)$_2$PO$_2$H and NaHCO$_3$ additives [75]. This prenylation could also occur under Ni(0) catalysis (**16g**) [76,77]. A distinct feature is that the formed five-membered metallacycle intermediate favorably undergoes oxidative addition with prenyl bromide/phosphate (**INT-14**), followed by reductive elimination to yield prenylated arenes.

Krische and colleagues documented an atom-economical approach for the synthesis of prenylated aromatics via iridium-catalyzed C–H addition of dimethylallene (**16h**) [78]. In this case, the *ortho* C–H bond is activated by oxidative addition with cationic Ir(I), followed by allene insertion into the Ir–H bond (**INT-15**) and reductive elimination to afford the target product. Mn(I) [79] and Rh(III) [80] could also promote directed C–H prenylation using dimethylallene (**16i,j**). Distinct to iridium catalysis, this process starts with CMD-type C–H activation, followed by allene insertion into the M–C bond (**INT-16**) and protonolysis to furnish the prenylated product.

Interestingly, Chen and coworkers showed that isoprene could be coupled with 2-arylpyridines and formaldehyde under Cp*Co(CO)I$_2$/AgSbF$_6$ catalysis (**17**) [81]. A directed CMD-type C–H activation of 2-phenylpyridine with cationic Co(III) yields a five-membered cobaltacycle. Subsequent migratory insertion of isoprene into the Co–C bond and β-hydrogen elimination lead to an oxidative coupling intermediate (**INT-17**). Further 1,4-insertion of an isoprene motif into a Co–H species generates a prenyl-Co(III) complex, followed by an addition with formaldehyde to deliver the desired product through a **Zimmerman–Traxler transition state** (**INT-18**). Independently, the groups of Ellman and Zhao reported similar results [82,83]. Currently, directed C–H prenylation generally occurs at the *ortho* position. It would be interesting to exploit suitable directing groups to achieve remote C–H prenylation of arenes.

By taking advantage of the inherent coordinating ability of azacycles, the laboratory of Hou unveiled a yttrium-catalyzed C–H addition of 2-ethylpyridine with isoprene, leading to prenylated and geranylated pyridines (**18a**, **19a**) in a molar ratio of 1.2:1 (Figure 6B) [84]. The half-sandwich bis(aminobenzyl) yttrium complex is first activated by B(C$_6$F$_5$)$_3$ to generate a cationic yttrium catalyst. A coordination of pyridine to the yttrium center aids *ortho*-C–H activation to deliver a three-membered yttrium cycle via release of *N,N*-dimethyl *o*-toluidine. Then, isoprene undergoes migratory insertion into the Y–C bond to yield a π-prenyl-yttrium species (**INT-19**). A final protonolysis results in the expected product. Analogously, Luo and Yao and colleagues prepared a zirconium dibenzyl complex with a tridentate [O,N,O] aniline-bridged bis(phenolato) ligand, which can promote the prenylation of 2-picoline in the presence of [Ph$_3$C][B(C$_6$F$_5$)$_4$] [85]. Compared with commonly used (*tert*-)prenyl electrophiles, such atom-economical C–H addition with isoprene to access prenylated products is more appealing.
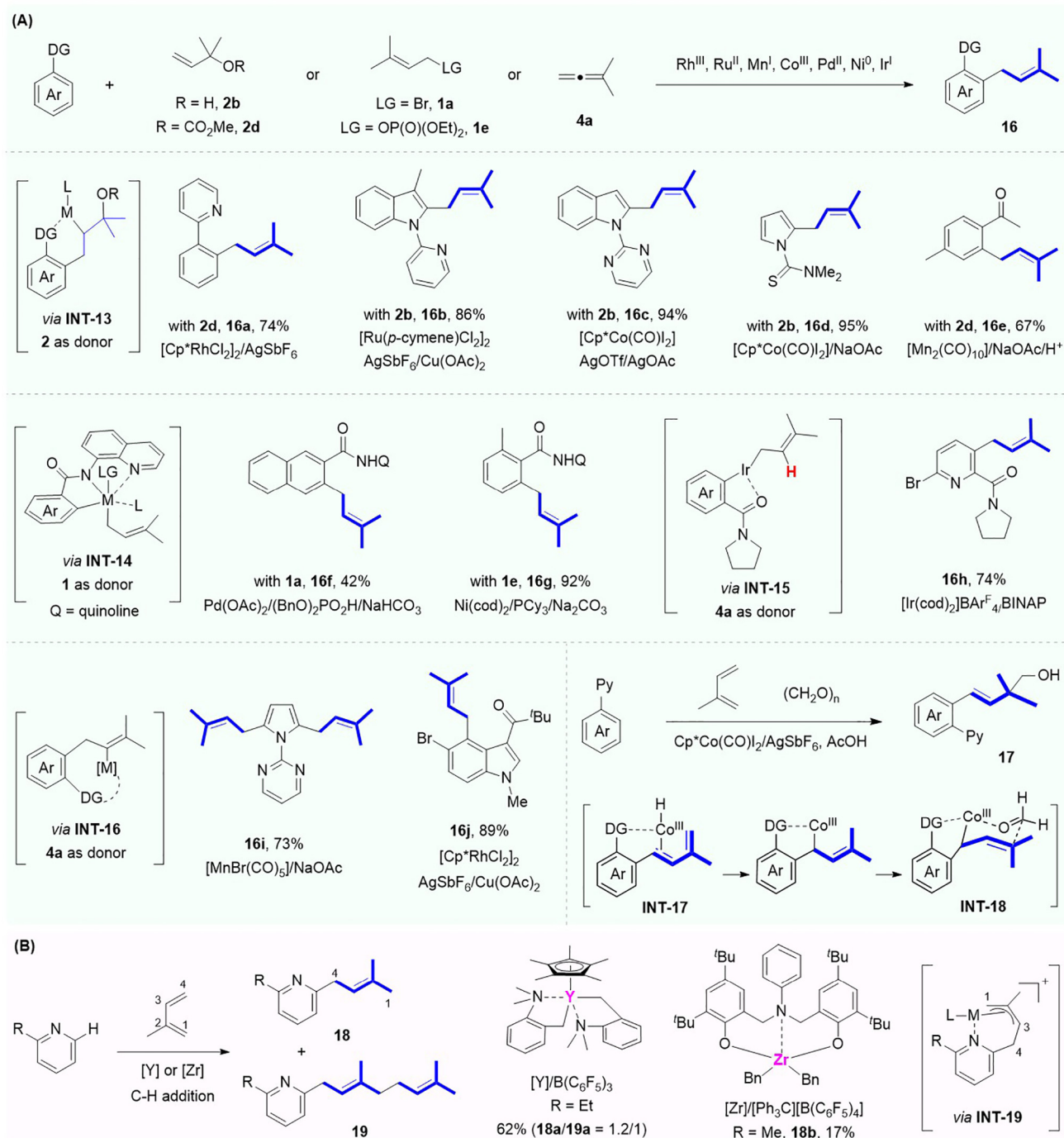
Figure 6. Catalytic prenylation and reverse prenylation of aromatics via C–H activation. (A) Directed C–H prenylation of aromatics. (B) C–H prenylation of pyridine with isoprene. Abbreviations: BAr$^F_4$, tetrakis[3,5-bis(trifluoromethyl)phenyl]boron; BINAP, 2,2'-bis(diphenylphosphino)-1,1'-binaphthalene; cod, 1,5-cyclooctadiene; Cp*, pentamethylcyclopentadienyl.

Catalytic prenylation and reverse prenylation of aromatics via nucleophilic attack at π-prenylmetals

By taking advantage of the nucleophilicity of indoles, the Tsuji–Trost reaction is another elegant strategy to introduce useful prenyl and reverse-prenyl groups. In 2005, Tamaru and coworkers reported the first C3 reverse prenylation of a simple indole using $Pd(PPh_3)_4$ as a catalyst and BEt_3 as a promoter (Figure 7A) [86]. It is suggested that BEt_3 is likely to interact with the nitrogen atom of indole to increase the nucleophilicity of the C3 position. Commercially available prenol proved to be a suitable partner and reverse-prenylated product **21a** (75%) was obtained exclusively. This strategy was successfully applied to install reverse-prenyl groups in the alkaloids hemiasterlin [87] and caulindole C [88].

Breit and colleagues showed that when using a diphenylphosphino pyridinone ligand, 6-DPPon$(CF_3)_2$ (**L4**), Pd-catalyzed reverse prenylation of indole with prenol occurred readily, and notably the additive BEt_3 was not required (Figure 7A) [89]. This ligand can interact with the hydroxyl group of prenol through hydrogen bonding, thereby promoting the release of the hydroxyl substituent and the formation of π-prenylpalladium species. Interestingly, Zhu's group demonstrated that with Lewis acid $MoO_2(acac)_2/NH_4PF_6$ as catalyst, the coupling of indole with prenol furnished 3-prenylindole **20a** via a π-prenylcation intermediate [90].

Pregosin and coworkers prepared a cationic ruthenium(IV) complex (**Ru-1**) via the reaction of $(Cp^*RuCl_2)_n$, allyl chloride, and $AgPF_6$ [91]. With this catalyst, the coupling between indole and *tert*-prenol offered reverse-prenylated product **21a** in 10:1 *rr* (Figure 7A). Encouraged by this work, the group of Bruneau used diphenylphosphinobenzene sulfonate as a source to incorporate a six-membered *P,O*-chelate onto a ruthenium center. The resulting complex **Ru-2** enhanced the regioselectivity to 19:1 [92].

Isoprene is electronically undifferentiated, rendering it more difficult to generate π-prenylmetal species and regulate the regioselectivity (Figure 7A; six addition modes in principle) [93]. In 2019, Chen and colleagues achieved prenylation and reverse prenylation of indoles with isoprene via **regiodivergent catalysis** [94]. The system comprising $Pd(PPh_3)_4$, the bulky ligand DTBM-Segphos, and BEt_3 enabled a facile synthesis of prenylated indole **20a** with high selectivity. By contrast, C3 reverse prenylation of an indole (**21a**) was found to be predominant when using $[Rh(cod)Cl]_2$, DTBM-Segphos, and Brønsted acid CSA as catalysts. Both transformations commence with the formation of metal-hydride species. The active Et_2B–Pd(II)–H catalyst is obtained via oxidative addition of BEt_3 with Pd(0) and further β-hydrogen elimination (-ethylene). An oxidative addition between acid CSA and Rh(I) yields active Rh(III)–H species. Subsequent migratory insertion of isoprene delivers π-prenylmetal species **INT-21**, followed by nucleophilic attack of indole and aromatization to produce the target products.

In 2013, Stanley and colleagues documented an efficient $[Pd(prenyl)Cl]_2$/Xantphos-catalyzed *N*-reverse prenylation of electron-deficient indole with *tert*-prenyl carbonate (**23a**) (Figure 7B) [95]. The electron-withdrawing groups could increase the acidity of NH, thus facilitating its nucleophilic attack onto the π-prenylpalladium(II) intermediate. This protocol has found applications in the preparation of marine alkaloid cyclomarin A with antimalarial properties [96].

Kim and coworkers reported that, with the assistance of $Pd(dba)_2$/Briphos and the co-acid catalyst C_6F_5OH, imidazole underwent *N*-prenylation with excellent yield and regioselectivity (**22b**) (Figure 7B) [97]. Briphos, a bicyclic bridgehead phosphoramidite ligand, possesses strong π-acceptor ability. This key feature together with hydrogen-bonding interactions between C_6F_5OH and hydroxyl in (*tert*-)prenol promote the oxidative addition step.

(See figure legend at the bottom of the next page.)
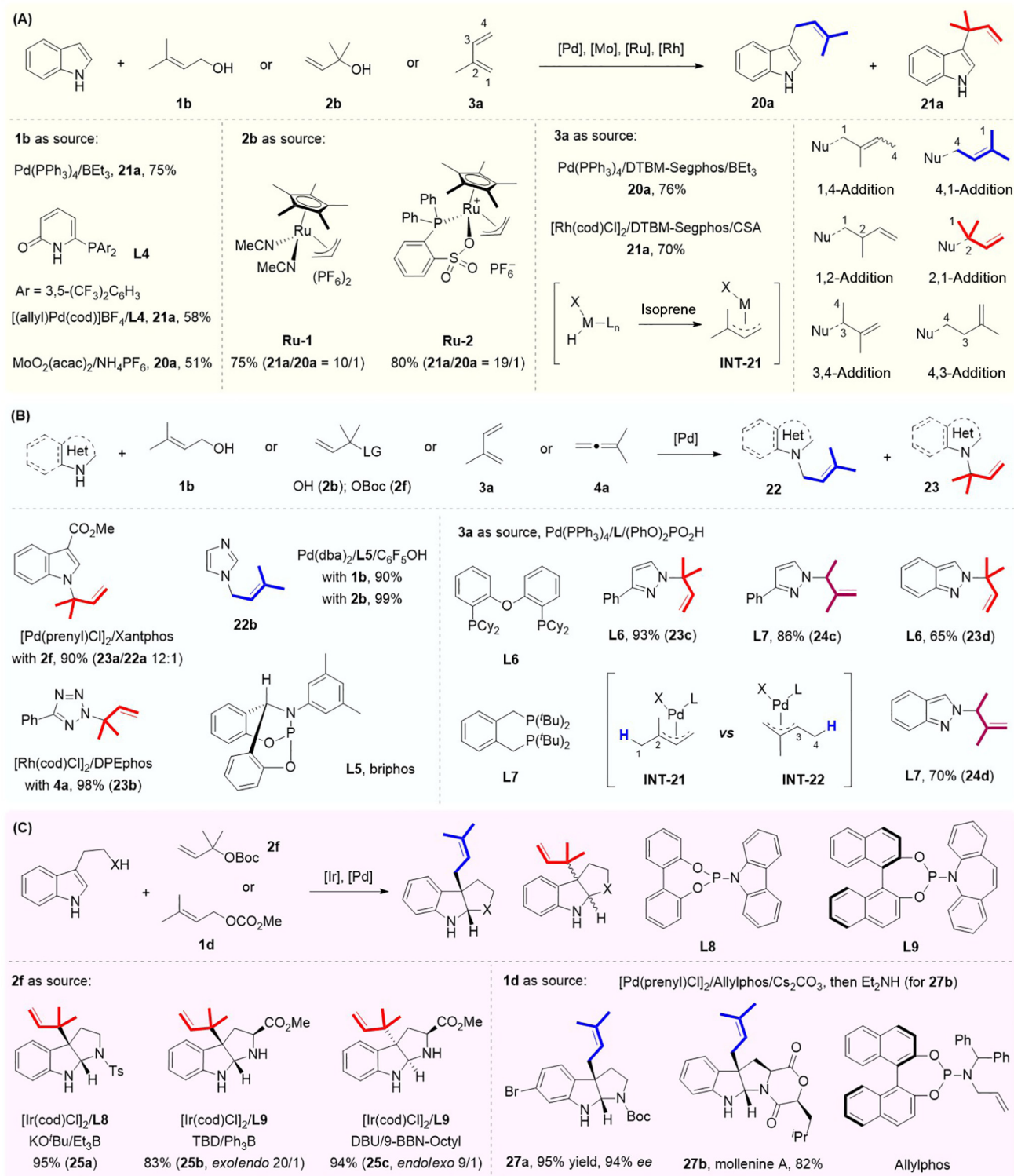
1,1-Dimethylallene is an effective prenyl source as well. In 2015, Breit and his colleagues accomplished reverse prenylation of tetrazole using 1,1-dimethylallene under [Rh(cod)Cl]$_2$/DPEphos catalysis (Figure 7B) [98]. The process commences with oxidative addition between NH of tetrazole and Rh(I) catalyst. Subsequent migratory insertion of allene into H-Rh-N species forms a π-prenyl-Rh-N complex, which further undergoes reductive elimination to produce *N*-reverse-prenylated product **23b**.

Recently, the group of Chen thoroughly investigated the regiodivergent coupling between pyrazoles/indazoles and isoprene under Pd–H catalysis (Figure 7B) [99]. With phosphoric acid as the additive, the coupling mainly occurred at the N2 position of pyrazoles/indazoles and the electrophilic reactive site of isoprene could be manipulated by the choice of ligand. The use of Cy-DPEphos (**L6**) led to 2,1 insertion of isoprene and N2 reverse-prenylated products (2,1-adducts, **23c**,**d**) were obtained exclusively (via **INT-21**). Conversely, 3,4-insertion of isoprene (3,4-adducts, **24c**,**d**) became a dominant pathway on variation to the bulky ligand **L7** (via **INT-22**). Independently, Dong and Yang and colleagues established one example of the reverse prenylation of pyrazole using isoprene under [Pd(allyl)Cl]$_2$/MeO-BIPHEP catalysis [100].

Carreira and his colleagues achieved the first dearomative C3 reverse prenylation of tryptamine derivatives (**25a**) using *tert*-prenyl carbonate (Figure 7C) [101]. A combination of [Ir(cod)Cl]$_2$ and phosphoramidite ligand (**L8**) efficiently promoted the reaction in the presence of KO^{t}Bu and BEt$_3$. Analogously, Stark and colleagues discovered a diastereodivergent dearomative C3 reverse prenylation of tryptophanate enabled by iridium and chiral phosphoramidite catalysis [102]. Both *exo* and *endo* products could be selectively obtained via tuning of the borane additive. For example, the reaction between Fmoc-*L*-Trp-OMe and *tert*-prenyl carbonate provided the *exo* product **25b** with 20:1 *dr* in the presence of Ph$_3$B, whereas the *endo* product **25c** proved to be predominant on changing to 9-BBN-octyl as the additive.

In 2018, an elegant enantioselective dearomative C3 prenylation of 3-substituted indoles was developed by You's group (Figure 7C) [103]. With [Pd(prenyl)Cl]$_2$ and chiral phosphoramidite ligand allylphos as catalysts, 6-bromo Boc-tryptamine reacted with prenyl carbonate well to afford product **27a** in 94% *ee*, which was a precursor of alkaloid (–)-flustramine B. Notably, L-tryptophan-based peptides were compatible with this process as well, followed by Et$_2$NH-promoted lactamization/lactonization to form *exo*-type indoline diketopiperazines (e.g., mollenine A, **27b**) with high diastereoselectivities.

Most of the known work employed biased (*tert*-)prenyl alcohols and their carbonates as the donors. It is because these activated precursors can selectively undergo oxidative addition with low-valent metals to furnish electrophilic π-prenylmetals. However, from an economic point of view, basic feedstock isoprene, which can also form π-prenylmetals under metal-hydride catalysis, is a more promising precursor. Accordingly, the exploration of prenylation and reverse prenylation of indoles with isoprene, as well as asymmetric versions, will be of great significance.

Figure 7. Catalytic prenylation and reverse prenylation of aromatics via nucleophilic attack at π-prenylmetals. (A) Catalytic C3 prenylation and reverse prenylation of simple indoles. (B) Catalytic *N*-prenylation and -reverse prenylation of various heterocycles. (C) Catalytic dearomative prenylation and reverse prenylation of 3-substituted indoles. (D) Representative alkaloids whose synthesis relies on prenylation and reverse prenylation of indoles. Abbreviations: 9-BBN-octyl, 9-octyl 9-borabicyclo[3.3.1]nonane; cod, 1,5-cyclooctadiene; CSA, camphor-10-sulfonic acid; dba, dibenzylideneacetone; DBU, 1,8-diazabicyclo[5.4.0]undec-7-ene; DPEphos, bis[(2-diphenylphosphino)phenyl] ether; DTBM-Segphos, 5,5′-bis[di(3,5-di-tert-butyl-4-methoxyphenyl)phosphino]-4,4′-bi-1,3-benzodioxole; PEG-6000, poly(ethylene glycol)-6000; TBD, 1,5,7-triazabicyclo[4,4,0]dec-5-ene; Xantphos, 4,5-bis(diphenylphosphino)-9,9-dimethylxanthene.

Trends in Chemistry

(See figure legend at the bottom of the next page.)
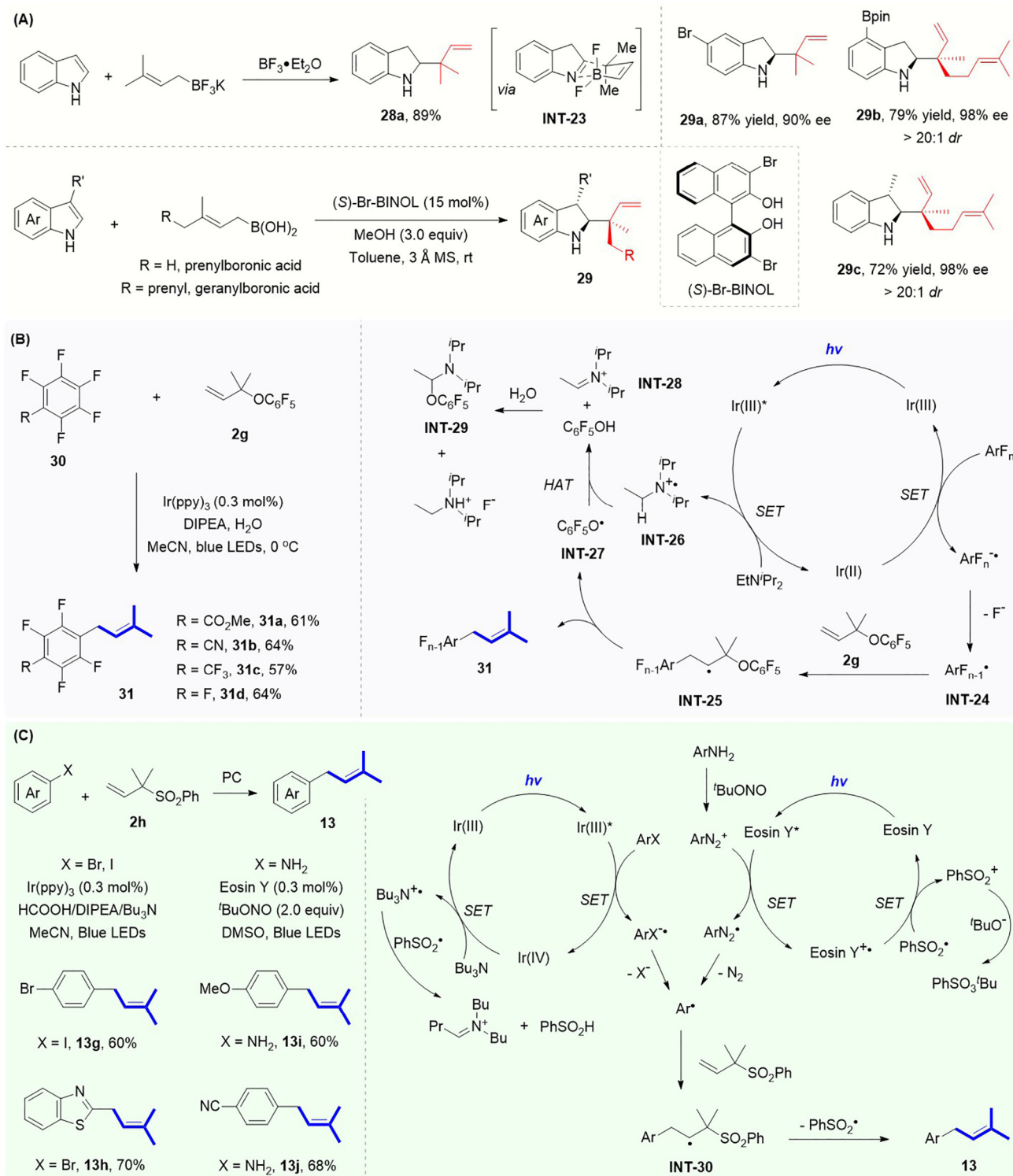
Catalytic reverse prenylation of indoles via addition reaction

The introduction of reverse-prenyl groups at the C2 position of indoles often depends on Danishefsky's multistep procedure [104–106]. By contrast, in 2013 Batey and colleagues unveiled a dearomative C2 reverse prenylation of indole with prenyltrifluoroborate (**28a**) in the presence of BF$_3$•Et$_2$O (Figure 8A) [107]. It is suggested that NH indole is first tautomerized into cyclic imine 3H-indole, which further undergoes addition with prenylboron difluoride species via Zimmerman–Traxler transition state **INT-23**. N-Methylindole, which cannot form a cyclic imine tautomer, was an ineffective substrate. Later, Szabó and coworkers established an asymmetric version with (S)-Br-BINOL as the catalyst [108]. A chiral BINOL-modified prenylboronate can be formed via the reaction of prenylboronic acid and the catalyst, followed by the same addition mode to give reverse-prenylated indoline (**29a**) with stereochemical induction. Notably, geranylboronic acid was amenable to the process as well and the branched products (**29b,c**) were afforded in high enantio- and diastereoselectivities.

Catalytic prenylation of aromatics via radical coupling

In 2018, Weaver and colleagues exploited a visible-light-induced Ir(III)-catalyzed C–F defluoroprenylation of perfluoroarenes in the presence of water and electron donor DIPEA (Figure 8B) [109]. The nature of the prenyl sources exerted a significant impact on the reaction and $tert$-prenyl pentafluorobenzene ether (**2g**) gave the best result. Electron-deficient groups on perfluorobenzene were well tolerated (**31a–d**) and the prenylation exclusively occurred at the $para$ position. Ir(ppy)$_3$ is first transformed into its **triplet excited state** under blue light-emitting diode (LED) irradiation, followed by **reductive quenching** with DIPEA to provide Ir(II) and amine radical cation **INT-26**. A single electron transfer (SET) of Ir(II) with perfluoroarene delivers perfluoroaryl radical anion with the regeneration of Ir(III). A subsequent extrusion of fluoride anion forms a perfluoroaryl radical (**INT-24**), which attacks at the alkene terminus of **2g** to yield radical **INT-25**. A further loss of pentafluorophenoxy radical (**INT-27**) delivers the desired prenylated product **31**.

Recently, the same group synthesized a bench-stable donor $tert$-prenyl sulfone **2h** via allylation of benzene sulfinate and dimethylation [110]. This reagent could undergo prenyl transfer to diverse aromatics under photoredox catalysis (Figure 8C). The prenylation of anilines occurred readily in the presence of the organic dye eosin Y and $tert$-butyl nitrite (^{t}BuONO), while a combination of Ir(ppy)$_3$, trialkylamine, and formic acid proved to be the optimal system for the prenylation of aryl halides. Both transformations start with the irradiation of the photocatalyst (PC) to give its excited state (PC*). Subsequent single electron transfer (SET) with aryldiazonium salts or aryl halides (**oxidative quenching**) yields aryl radical with the loss of nitrogen or halide anions. Further addition with $tert$-prenyl sulfone generates radical **INT-30**, followed by elimination of the sulfonyl radical to obtain the desired prenylarenes **13**. The oxidized form of the PC is reduced by trialkylamine and the sulfonyl radical to regenerate the Ir(ppy)$_3$ and eosin Y, respectively. It is worth mentioning that reductive quenching cycle of excited PCs cannot be ruled out.

Concluding remarks

To conclude, chemical catalytic prenylation and reverse-prenylation of aromatics have witnessed significant progress over the past decades. Feasible strategies include the Friedel–Crafts reaction, cross-coupling, C–H bond activation, Tsuji–Trost-like reactions, addition reactions, and radical coupling. Their utility has been highlighted in the total synthesis of diverse natural alkaloids.

Figure 8. Catalytic prenylation and reverse prenylation of aromatics via addition and radical reaction. (A) Catalytic C2 reverse prenylation of indoles via addition reaction. (B) Photocatalytic defluoroprenylation of perfluoroarenes. (C) Photocatalytic prenylation of arenes with $tert$-prenyl sulfones. Abbreviations: DIPEA, N,N-diisopropylethylamine; DMSO, dimethyl sulfoxide; HAT, hydrogen atom transfer; Ir(ppy)$_3$, tris(2-phenylpyridine)iridium; LED, light-emitting diode; SET, single electron transfer.

Outstanding questions

Will bulk chemical isoprene become a versatile precursor for the incorporation of prenyl and reverse-prenyl groups?

How can we realize enantioselective prenylation and reverse prenylation of aromatics with isoprene?

How can we achieve selective geranylation of aromatics with isoprene?

Is it possible to install prenyl and reverse-prenyl groups onto the benzenoid ring of indoles via a C–H activation strategy?

Will prenylation and reverse prenylation find applications in the late-stage modification of medically relevant molecules?

Trends in Chemistry

Press

Dimethylallylic (prenyl versus *tert*-prenyl) alcohols and their derivatives, homoallyl alcohol, isoprene, and dimethylallene as well as 2-methyl-2-butene are versatile precursors. Because of the steric hindrance, prenylation is achieved in most cases, whereas reverse-prenylation can be attained only via careful tuning of transition-metal catalysts and ligands.

From the viewpoint of step and atom economy, bulk chemical isoprene is an ideal prenyl source. However, electronically unbiased isoprene might lead to six possible regioisomers. Owing to this challenging issue, (reverse) prenylation using isoprene remains in its infancy (see Outstanding questions). Future efforts will be devoted to developing common strategies to manipulate the regioselectivity (regiodivergent catalysis). There will also be plenty of room for the development of enantioselective dearomative (reverse) prenylations of indoles with isoprene. Since sometimes geranylated product could also be obtained in prenylation reactions (Figure 6B), it will be highly desirable to exploit suitable catalytic systems to realize selective geranylation of aromatics with isoprene.

Indoles with prenyl and reverse-prenyl groups on the benzenoid ring are also widely distributed in natural alkaloids and their synthesis often relies on enzymatic catalysis. With chemical catalysis, current (reverse) prenylation of indoles generally takes place at N, C2, and C3 positions. In contrast, direct C–H (reverse)prenylation of the benzenoid ring of indole remains underexplored. In this context, exploiting suitable directing groups to achieve this goal will be an important research area.

Catalytic late-stage functionalization is arguably the simplest tool to quickly modulate the properties of a lead compound without the need for *de novo* synthesis, which will certainly accelerate the discovery of new drugs. Additional attention will be directed towards exploring the late-stage (reverse) prenylation of medically relevant molecules, since the presence of (reverse) prenyl units can improve their interactions with target proteins.

Declaration of interests

The authors declare no interests.

References

1. Oldfield, E. and Lin, F.Y. (2012) Terpene biosynthesis: modularity rules. *Angew. Chem. Int. Ed.* 51, 1124–1137
2. Lindel, T. *et al.* (2011) Indole prenylation in alkaloid synthesis. In *Alkaloid synthesis. Topics in current chemistry* (309) (Knölker, H.J., ed.), pp. 67–129, Springer
3. Burlison, J.A. *et al.* (2006) Novobiocin: redesigning a DNA gyrase inhibitor for selective inhibition of Hsp90. *J. Am. Chem. Soc.* 128, 15529–15536
4. Wang, H.-J. *et al.* (1998) Mollenines A and B: new dioxomorpholines from the ascostromata of *Eupenicillium molle*. *J. Nat. Prod.* 61, 804–807
5. Yao, J. *et al.* (2015) Xanthohumol, a polyphenol chalcone present in hops, activating Nrf2 enzymes to confer protection against oxidative damage in PC12 cells. *J. Agric. Food Chem.* 63, 1521–1531
6. Sprogøe, K. *et al.* (2005) Janoxepin and brevicompanine B: antiplasmodial metabolites from the fungus *Aspergillus janus*. *Tetrahedron* 61, 8718–8721
7. Cardellina, J.H. *et al.* (1979) Seaweed dermatitis: structure of lyngbyatoxin A. *Science* 204, 193–195
8. de Bruijn, W.J.C. *et al.* (2020) Plant aromatic prenyltransferases: tools for microbial cell factories. *Trends Biotechnol.* 38, 917–934
9. Tanner, M.E. (2015) Mechanistic studies on the indole prenyltransferases. *Nat. Prod. Rep.* 32, 88–101
10. Caballero, E. *et al.* (2003) Brief total synthesis of the cell cycle inhibitor tryprostatin B and related preparation of its alanine analogue. *J. Org. Chem.* 68, 6944–6951
11. Khopade, T.M. *et al.* (2021) Bioinspired Brønsted acid-promoted regioselective tryptophan isoprenylations. *ACS Omega* 6, 10840–10858
12. Depew, K.M. *et al.* (1996) Total synthesis of tryprostatin B: generation of a nucleophilic prenylating species from a prenylstannane. *J. Am. Chem. Soc.* 118, 12463–12464
13. Zhao, S. *et al.* (1998) Total synthesis of tryprostatin A and B as well as their enantiomers. *Tetrahedron Lett.* 39, 7009–7012
14. Huisman, M. *et al.* (2019) Total synthesis of tryprostatin B: synthesis and asymmetric phase-transfer-catalyzed reaction of prenylated gramine salt. *Org. Lett.* 21, 134–137
15. Hu, Y.-C. *et al.* (2021) Catalytic C2 prenylation of unprotected indoles: late-stage diversification of peptides and two-step total synthesis of tryprostatin B. *Chin. J. Catal.* 42, 1593–1607
16. Malkov, A.V. *et al.* (1999) Molybdenum(II)-catalyzed allylation of electron-rich aromatics and heteroaromatics. *J. Org. Chem.* 64, 2751–2764

17. Judd, K.E. and Caggiano, L. (2011) Bi(OTf)$_3$-catalysed prenylation of electron-rich aryl ethers and phenols with isoprene: a direct route to prenylated derivatives. *Org. Biomol. Chem.* 9, 5201–5210

18. Cacciuttolo, B. *et al.* (2014) Bi(OTf)$_3$-catalysed synthesis of substituted indanes by a double hydroarylation of unactivated 1,3-dienes. *Org. Chem. Front.* 1, 765–769

19. Villani-Gale, A.J. and Eichman, C.C. (2016) Iron-catalyzed arene prenylation. *Eur. J. Org. Chem.* 2016, 2925–2928

20. Niggemann, M. and Meel, M.J. (2010) Calcium-catalyzed Friedel–Crafts alkylation at room temperature. *Angew. Chem. Int. Ed.* 49, 3684–3687

21. Ricardo, C.L. *et al.* (2015) A surprising substituent effect provides a superior boronic acid catalyst for mild and metal-free direct Friedel–Crafts alkylations and prenylations of neutral arenes. *Chem. Eur. J.* 21, 4218–4223

22. Tarselli, M.A. *et al.* (2009) Gold(I)-catalyzed intermolecular hydroarylation of allenes with nucleophilic arenes: scope and limitations. *Tetrahedron* 65, 1785–1789

23. Kayaki, Y. *et al.* (2004) A highly effective (triphenyl phosphite) palladium catalyst for a cross-coupling reaction of allylic alcohols with organoboronic acids. *Eur. J. Org. Chem.* 2004, 4989–4993

24. Manabe, K. *et al.* (2005) Cross-coupling reactions of allylic alcohols in water. *Adv. Synth. Catal.* 347, 1499–1503

25. Singh, R. *et al.* (2005) Simple (imidazol-2-ylidene)-Pd-acetate complexes as effective precatalysts for sterically hindered Suzuki–Miyaura couplings. *Org. Lett.* 7, 1829–1832

26. Ye, J. *et al.* (2013) Pd-catalyzed stereospecific allyl-aryl coupling of allylic alcohols with arylboronic acids. *Chem. Commun.* 49, 9761–9763

27. Levin, M.D. and Toste, F.D. (2014) Gold-catalyzed allylation of aryl boronic acids: accessing cross-coupling reactivity with gold. *Angew. Chem. Int. Ed.* 53, 6211–6215

28. Mayer, M. *et al.* (2010) Practical iron-catalyzed allylations of aryl Grignard reagents. *Adv. Synth. Catal.* 352, 2147–2152

29. Kalkan, M. and Erdik, E. (2016) Reactivity of mixed organozinc and mixed organocopper reagents: 14. Phosphine-nickel catalyzed aryl–allyl coupling of (n-butyl)(aryl)zincs. Ligand and substrate control on the group selectivity and regioselectivity. *J. Organomet. Chem.* 818, 28–36

30. Ma, E. *et al.* (2018) Salicylate-directed C–O bond cleavage: iron-catalyzed allylic substitution with Grignard reagents. *Asian J. Org. Chem.* 7, 914–917

31. Leister, J. *et al.* (2021) Palladium-catalyzed prenylation of (hetero)aryl boronic acids. *Tetrahedron Lett.* 66, 152800

32. Takemura, S. *et al.* (1999) A concise total synthesis of (±)-A80915G, a member of the napyradiomycin family of antibiotics. *Tetrahedron Lett.* 40, 7501–7505

33. Shiozawa, M. *et al.* (2018) Synthesis of 2,6,7-trisubstituted prenylated indole. *J. Org. Chem.* 83, 7276–7280

34. Hatanaka, Y. *et al.* (1991) γ-Selective cross-coupling reaction of allyltrifluorosilanes: a new approach to regiochemical control in allylic systems. *J. Am. Chem. Soc.* 113, 7075–7076

35. Hatanaka, Y. *et al.* (1994) α-Selective cross-coupling reaction of allyltrifluorosilanes: remarkable ligand effect on the regiochemistry. *Tetrahedron Lett.* 35, 6511–6514

36. Gerbino, D.C. *et al.* (2009) Introduction of allyl and prenyl side-chains into aromatic systems by Suzuki cross-coupling reactions. *Eur. J. Org. Chem.* 2009, 3964–3972

37. Lee, P.H. *et al.* (2001) Palladium-catalyzed cross-coupling reactions of *in situ* generated allylindium reagents with aryl halides. *Org. Lett.* 3, 3201–3204

38. Dai, Q. *et al.* (2011) Total syntheses of tardioxopiperazine A, isoechinulin A, and variecolorin C. *Org. Lett.* 13, 2302–2305

39. Farmer, J.L. *et al.* (2012) Regioselective cross-coupling of allylboronic acid pinacol ester derivatives with aryl halides via Pd-PEPPSI-IPent. *J. Am. Chem. Soc.* 134, 17470–17473

40. Ellwart, M. and Knochel, P. (2015) Preparation of solid, substituted allylic zinc reagents and their reactions with electrophiles. *Angew. Chem. Int. Ed.* 54, 10662–10665

41. Yang, Y. *et al.* (2013) Palladium-catalyzed completely linear-selective Negishi cross-coupling of allylzinc halides with aryl and vinyl electrophiles. *Angew. Chem. Int. Ed.* 52, 14098–14102

42. Yang, Y. and Buchwald, S.L. (2013) Ligand-controlled palladium-catalyzed regiodivergent Suzuki–Miyaura cross-coupling of allylboronates and aryl halides. *J. Am. Chem. Soc.* 135, 10642–10645

43. Thomas, C. *et al.* (2014) Regioselective prenylation of bromocarbazoles by palladium(0)-catalysed cross coupling: synthesis of *O*-methylsiamenol, *O*-methylmicromeline and carquinostatin A. *Org. Biomol. Chem.* 12, 872–875

44. Shen, R. *et al.* (2003) Lobatamide C: total synthesis, stereochemical assignment, preparation of simplified analogues, and V-ATPase inhibition studies. *J. Am. Chem. Soc.* 125, 7889–7901

45. Pirrung, M.C. *et al.* (2005) Methyl scanning: total synthesis of demethylasterriquinone B1 and derivatives for identification of sites of interaction with and isolation of its receptor(s). *J. Am. Chem. Soc.* 127, 4609–4624

46. Godfrey, N.A. *et al.* (2018) Twelve-step asymmetric synthesis of (-)-nodulisporic acid C. *J. Am. Chem. Soc.* 140, 12770–12774

47. Tang, Y. *et al.* (2017) Collective syntheses of 2-(3-methylbenzofuran-2-yl)phenol-derived natural products by a cascade [3,3]-sigmatropic rearrangement/aromatization strategy. *J. Org. Chem.* 82, 11102–11109

48. Mikusek, J. *et al.* (2018) Synthetic studies on the natural product myrsinoic acid F reveal biologically active analogues. *Org. Lett.* 20, 3984–3987

49. Bartoccini, F. *et al.* (2019) Total synthesis of (-)-clavicipitic acid via γ,γ-dimethylallyltryptophan (DMAT) and chemoselective C–H hydroxylation. *J. Org. Chem.* 84, 8027–8034

50. Shi, S. *et al.* (2020) Seven-step total synthesis of α-cyclopiazonic acid. *Chin. Chem. Lett.* 31, 401–403

51. Pan, X. and Liu, Z. (2019) Total synthesis and antibacterial activity evaluation of griseofamine A and 16-epi-griseofamine A. *Org. Lett.* 21, 2393–2396

52. Wang, H. and Reisman, S.E. (2014) Enantioselective total synthesis of (-)-lansai B and (+)-nocardioazines A and B. *Angew. Chem. Int. Ed.* 53, 6206–6210

53. Hayashi, S. *et al.* (2006) Palladium-catalyzed stereo- and regiospecific allylation of aryl halides with homoallyl alcohols via retro-allylation: selective generation and use of σ-allylpalladium. *J. Am. Chem. Soc.* 128, 2210–2211

54. Iwasaki, M. *et al.* (2007) Pd(OAc)$_2$/P(^{c}C$_6$H$_{11}$)$_3$-catalyzed allylation of aryl halides with homoallyl alcohols via retro-allylation. *J. Am. Chem. Soc.* 129, 4463–4469

55. Ohmiya, H. *et al.* (2008) Palladium-catalyzed γ-selective and stereospecific allyl–aryl coupling between allylic acetates and arylboronic acids. *J. Am. Chem. Soc.* 130, 17276

56. Ohmiya, H. *et al.* (2010) Palladium-catalyzed γ-selective and stereospecific allyl–aryl coupling between acyclic allylic esters and arylboronic acids. *J. Am. Chem. Soc.* 132, 879–889

57. Makida, Y. *et al.* (2011) Sulfonamidoquinoline/palladium(II)-dimer complex as a catalyst precursor for palladium-catalyzed γ-selective and stereospecific allyl–aryl coupling reaction between allylic acetates and arylboronic acids. *Chem. Asian J.* 6, 410–414

58. Cui, X. *et al.* (2013) Nickel-catalyzed reductive allylation of aryl bromides with allylic acetates. *Org. Biomol. Chem.* 11, 3094–3097

59. Jia, X.-G. *et al.* (2018) Dual nickel and Lewis acid catalysis for cross-electrophile coupling: the allylation of aryl halides with allylic alcohols. *Chem. Sci.* 9, 640–645

60. Luzung, M.R. *et al.* (2009) Direct, chemoselective *N-tert*-prenylation of indoles by C–H functionalization. *Angew. Chem. Int. Ed.* 48, 7025–7029

61. Kim, D.E. *et al.* (2019) Total synthesis of paspaline A and emindole PB enabled by computational augmentation of a transform-guided retrosynthetic strategy. *J. Am. Chem. Soc.* 141, 1479–1483

62. Choules, M.P. *et al.* (2018) Residual complexity does impact organic chemistry and drug discovery: the case of rufomyazine and rufomycin. *J. Org. Chem.* 83, 6664–6672

63. Cheng, Y. *et al.* (2018) Total synthesis of anti-tuberculosis natural products ilamycins E$_1$ and F. *Org. Lett.* 20, 6166–6169

64. Barbie, P. and Kazmaier, U. (2016) Total synthesis of desoxycyclomarin C and the cyclomarazines A and B. *Org. Biomol. Chem.* 14, 6055–6064

65. Wang, H. *et al.* (2013) Mild rhodium(III)-catalyzed direct C–H allylation of arenes with allyl carbonates. *Angew. Chem. Int. Ed.* 52, 5386–5389

66. Debbarma, S. *et al.* (2016) Cp*Rh(III)-catalyzed low temperature C–H allylation of *N*-aryl-trichloro acetimidamide. *J. Org. Chem.* 81, 11716–11725

67. Wu, X. and Ji, H. (2018) Rhodium(III)-catalyzed C–H allylation of indoles with allyl alcohols via β-hydroxide elimination. *Org. Biomol. Chem.* 16, 5691–5698

68. Jo, H. *et al.* (2016) Rhodium(III)-catalyzed heteroatom-directed C–H allylation with allylic phosphonates and allylic carbonates at room temperature. *Tetrahedron* 72, 571–578

69. Kim, M. *et al.* (2014) Direct allylation of aromatic and α,β-unsaturated carboxamides under ruthenium catalysis. *Chem. Commun.* 50, 11303–11306

70. Kumar, G.S. and Kapur, M. (2016) Ruthenium-catalyzed, site-selective C–H allylation of indoles with allyl alcohols as coupling partners. *Org. Lett.* 18, 1112–1115

71. Suzuki, Y. *et al.* (2015) Dehydrative direct C–H allylation with allylic alcohols under [Cp*Co^{III}] catalysis. *Angew. Chem. Int. Ed.* 54, 9944–9947

72. Bunno, Y. *et al.* (2016) Cp*Co^{III}-catalyzed dehydrative C–H allylation of 6-arylpurines and aromatic amides using allyl alcohols in fluorinated alcohols. *Org. Lett.* 18, 2216–2219

73. Basuli, S. *et al.* (2021) Cp*Co(III)-catalyzed dehydrative C2-prenylation of pyrrole and indole with allyl alcohols. *Adv. Synth. Catal.* 363, 4605–4611

74. Liu, W. *et al.* (2016) Manganese(I)-catalyzed substitutive C–H allylation. *Angew. Chem. Int. Ed.* 55, 7747–7750

75. Zhang, S.-Y. *et al.* (2015) Pd-catalyzed monoselective *ortho*-C–H alkylation of *N*-quinolyl benzamides: evidence for stereoretentive coupling of secondary alkyl iodides. *J. Am. Chem. Soc.* 137, 531–539

76. Cong, X. *et al.* (2014) Nickel-catalyzed C–H coupling with allyl phosphates: a site-selective synthetic route to linear allylarenes. *Org. Lett.* 16, 3926–3929

77. Barsu, N. *et al.* (2015) Carboxylate assisted Ni-catalyzed C–H bond allylation of benzamides. *Chem. Eur. J.* 21, 9364–9368

78. Zhang, Y. *et al.* (2009) Direct prenylation of aromatic and α,β-unsaturated carboxamides via iridium-catalyzed C–H oxidative addition-allene insertion. *Org. Lett.* 11, 4248–4250

79. Chen, S.-Y. *et al.* (2017) Manganese(I)-catalyzed direct C–H allylation of arenes with allenes. *J. Org. Chem.* 82, 11173–11181

80. Zhang, S.-S. *et al.* (2022) Rhodium(III)-catalyzed regioselective C–H allylation and prenylation of indoles at C4-position. *Adv. Synth. Catal.* 364, 64–70

81. Yang, J. *et al.* (2019) Cobalt-catalyzed hydroxymethylarylation of terpenes with formaldehyde and arenes. *Chem. Sci.* 10, 9560–9564

82. Li, R. *et al.* (2019) Rhodium(III) vs. cobalt(III): a mechanistically distinct three-component C–H bond addition cascade using a Cp*Rh^{III} catalyst. *Chem. Commun.* 55, 695–698

83. Dongbang, S. *et al.* (2012) Synthesis of homoallylic alcohols with acyclic quaternary centers through Co^{III}-catalyzed three-component C–H bond addition to internally substituted dienes and carbonyls. *Angew. Chem. Int. Ed.* 58, 12590–12594

84. Guan, B.-T. and Hou, Z. (2011) Rare-earth-catalyzed C–H bond addition of pyridines to olefins. *J. Am. Chem. Soc.* 133, 18086–18089

85. Sun, Q. *et al.* (2018) Addition of C–H bonds of pyridine derivatives to alkenes catalyzed by zirconium complexes bearing amine-bridged bis(phenolato) ligands. *Inorg. Chem.* 57, 11788–11800

86. Kimura, M. *et al.* (2005) Pd-catalyzed C3-selective allylation of indoles with allyl alcohols promoted by triethylborane. *J. Am. Chem. Soc.* 127, 4592–4593

87. Lang, J.H. *et al.* (2017) Total synthesis of the marine natural product hemiasterlin by organocatalyzed α-hydrazination. *Chem. Eur. J.* 23, 12714–12717

88. Dethe, D.H. *et al.* (2014) Remarkable switch of regioselectivity in Diels–Alder reaction: divergent total synthesis of borreverine, caulindoles, and flinderoles. *Org. Lett.* 16, 2764–2767

89. Usui, L. *et al.* (2008) Allylation of *N*-heterocycles with allylic alcohols employing self-assembling palladium phosphane catalysts. *Org. Lett.* 10, 1207–1210

90. Yang, H. *et al.* (2009) An efficient molybdenum(VI)-catalyzed direct substitution of allylic alcohols with nitrogen, oxygen, and carbon nucleophiles. *Eur. J. Org. Chem.* 2009, 666–672

91. Gruber, S. *et al.* (2008) Facile ruthenium(IV)-catalyzed single and double allylation of indole compounds using alcohols as substrates: aspects of ruthenium(IV) allyl chemistry. *Organometallics* 27, 3796–3805

92. Sundararaju, B. *et al.* (2010) Ruthenium(IV) complexes featuring P,O-chelating ligands: regioselective substitution directly from allylic alcohols. *Angew. Chem. Int. Ed.* 49, 2782–2785

93. Zhang, W.-S. *et al.* (2020) Isoprene: a promising coupling partner in C–H functionalizations. *Synlett* 31, 1649–1655

94. Hu, Y.-C. *et al.* (2019) Catalytic prenylation and reverse prenylation of indoles with isoprene: regioselectivity manipulation through choice of metal hydride. *Angew. Chem. Int. Ed.* 58, 5438–5442

95. Johnson, K.F. *et al.* (2013) Palladium-catalyzed synthesis of *N-tert*-prenylindoles. *Org. Lett.* 15, 2798–2801

96. Barbie, P. and Kazmaier, U. (2016) Total synthesis of cyclomarin A, a marine cycloheptapeptide with anti-tuberculosis and anti-malaria activity. *Org. Lett.* 18, 204–207

97. Kang, K. *et al.* (2016) Palladium-catalyzed dehydrative cross-coupling of allylic alcohols and *N*-heterocycles promoted by a bicyclic bridgehead phosphoramidite ligand and an acid additive. *Org. Lett.* 18, 616–619

98. Xu, K. *et al.* (2015) Enantioselective formation of tertiary and quaternary allylic C–N bonds via allylation of tetrazoles. *Chem. Commun.* 51, 10861–10863

99. Jiang, W.-S. *et al.* (2021) Orthogonal regulation of nucleophilic and electrophilic sites in Pd-catalyzed regiodivergent couplings between indazoles and isoprene. *Angew. Chem. Int. Ed.* 60, 8321–8328

100. Jiu, A.Y. *et al.* (2021) Enantioselective addition of pyrazoles to dienes. *Angew. Chem. Int. Ed.* 60, 19660–19664

101. Ruchti, J. and Carreira, E.M. (2014) Ir-catalyzed reverse prenylation of 3-substituted indoles: total synthesis of (+)-aszonalenin and (-)-brevicompanine B. *J. Am. Chem. Soc.* 136, 16756–16759

102. Müller, J.M. and Stark, C.B.W. (2016) Diastereodivergent reverse prenylation of indole and tryptophan derivatives: total synthesis of amauromine, novoamauromine, and epi-amauromine. *Angew. Chem. Int. Ed.* 55, 4798–4802

103. Tu, H.-F. *et al.* (2018) Enantioselective dearomative prenylation of indole derivatives. *Nat. Catal.* 1, 601–608

104. Schkeryantz, J.M. *et al.* (1999) Total synthesis of gypsetin, deoxybrevianamide E, brevianamide E, and tryprostatin B: novel constructions of 2,3-disubstituted indoles. *J. Am. Chem. Soc.* 121, 11964–11975

105. Zhao, L. *et al.* (2012) Stereoselective synthesis of brevianamide E. *Org. Lett.* 14, 90–93

106. Godfrey, R.C. *et al.* (2020) Total synthesis of brevianamide A. *Nat. Chem.* 12, 615–619

107. Nowrouzi, F. and Batey, R.A. (2013) Regio- and stereoselective allylation and crotylation of indoles at C2 through the use of potassium organotrifluoroborate salts. *Angew. Chem. Int. Ed.* 52, 892–895

108. Alam, R. *et al.* (2016) Catalytic asymmetric allylboration of indoles and dihydroisoquinolines with allylboronic acids: stereodivergent synthesis of up to three contiguous stereocenters. *Angew. Chem. Int. Ed.* 55, 14417–14421

109. Priya, S. and Weaver, J.D. (2018) Prenyl praxis: a method for direct photocatalytic defluoroprenylation. *J. Am. Chem. Soc.* 140, 16020–16025

110. Rathnayake, M.D. and Weaver, J.D. (2020) A general photocatalytic route to prenylation. *Eur. J. Org. Chem.* 2020, 1433–1438